ORIGINAL ARTICLE

A novel antitumor piperazine alkyl compound causes apoptosis by inducing RhoB expression via ROS-mediated c-Abl/p38 MAPK signaling

Kyung-Sook Chung · Gyoonhee Han · Bo-Kyung Kim · Hwan-Mook Kim · Jee Sun Yang · Jiwon Ahn · Kyeong Lee · Kyung-Bin Song · Misun Won

Abstract

Purpose We investigated the action mechanism of a novel anticancer compound, KR28 (1-allyl-4-dodecanoyl-1-ethyl-piperazin-1-ium; bromide), to induce apoptosis of human prostate carcinoma PC-3 cells.

Methods To explore an apoptotic signaling of KR28, we used ROS assay, SRB assay, flow cytometry analysis, reporter assay, xenograft assay, Western blotting, and RT-PCR analysis.

Results The growth inhibitory action of KR28 is cell line specific, impeding the growth of prostate carcinoma PC-3 and stomach carcinoma NUGC-3 cells. KR28 showed strong antitumor activity in PC-3 mouse xenograft model. KR28 increased ROS production, leading to nuclear c-Abl expression, which in turn activated p38 mitogen-activated protein kinase (MAPK) to enhance the expression of RhoB, an apoptosis inducer. The KR28-induced apoptosis was abrogated by the ROS scavenger N-acetylcysteine and by knockdown of c-Abl, p38 MAPK, or ATF2. Moreover, the p300 binding site and two CCAAT boxes in the RhoB promoter appear to be involved in ROS-mediated RhoB expression in the presence of KR28.

Conclusion The antitumor agent KR28 induces apoptosis of PC-3 cells by ROS-mediated RhoB expression via c-Abl upregulation and activation of p38 MAPK/ATF-2.

Keywords Prostate cancer · RhoB · ROS · c-Abl · p38 MAPK

Abbreviations

ROS	Reactive oxygen species
NAC	N-acetyl cysteine
MAPK	Mitogen-activated protein kinase
SAPK/JNK	Stress-activated protein kinase/c-Jun N-terminal kinase
PI3K	Phosphoinositide 3-kinase
FTI	Farnesyltransferase inhibitor
SRB	Sulforhodamine B

Kyung-Sook Chung, Gyoonhee Han and Bo-Kyung Kim have contributed equally to this work.

K.-S. Chung · B.-K. Kim · J. Ahn · M. Won (✉)
Medical Genome Research Center, KRIBB, Yusong,
Daejeon 305-806, Korea
e-mail: misun@kribb.re.kr

K.-S. Chung · M. Won
Functional Genomics, University of Science and Technology,
Daejeon 305-350, Korea

G. Han · J. S. Yang
Department of Biotechnology, Yonsei University,
Seoul 129-749, Korea

H.-M. Kim
College of Pharmacy, Gachon University,
Incheon 406-840, Korea

K. Lee
College of Pharmacy, Dongguk University, Gyeongju,
Kyungki-do 410-773, Korea

K.-B. Song
Department of Food Science and Technology,
Chungnam National University, Daejon 305-764, Korea

Introduction

In cancer cells, the increase in ROS plays an important role in the initiation and progression, but excessive levels of ROS stress can be toxic, resulting in apoptosis [1, 2]. The reactive oxygen species (ROS) are caused by oxidative stress through mitochondrial metabolism, ER stress, exogenous chemotherapeutic reagents, and other unknown mechanisms [3, 4]. ROS activates nuclear c-Abl tyrosine kinase, which is implicated in mechanisms of DNA damage dependent in part on p53 and its homolog, p73 [5, 6]. The c-Abl activates the p38 mitogen-activated protein kinase (MAPK) and the c-Jun N-terminal kinase (SAPK/JNK) pathways [7, 8]. Also, c-Abl phosphorylates the p85 subunit of PI3 K to inhibit Akt in the apoptotic response [9].

RhoB expression is reduced in most invasive tumors with loss of RhoB expression correlating significantly with tumor stage [10]. RhoB antagonizes the epithelial growth factor receptor (EGFR) and downregulates the Ras/PI3K/Akt pathway [11], thereby inhibiting the growth and survival, transformation, migration, invasion, and metastasis of cells. RhoB induces apoptosis in various cancer cells and is suggested as a therapeutic target in various cancers [12, 13]. The expression of RhoB is induced by radiation, growth factors, cytokines, and genotoxic stress [4, 14, 15]. Farnesyltransferase inhibitors (FTIs) induce ROS-mediated RhoB expression through histone acetylation of the RhoB promoter by ATF-2 interaction with the CCAAT-binding factor, NF-YA, at the inverted CCAAT (iCCAAT) box [15, 16].

NSC126188 induced apoptosis by increasing RhoB expression via JNK-mediated signaling in NUGC-3 cells [17, 18]. In search of novel anticancer agents, derivatives of NSC126188 have thus been synthesized and screened for inhibition of malignant cell growth. We report here a novel compound, KR28 (1-allyl-4-dodecanoyl-1-ethyl-piperazin-1-ium; bromide), which is highly effective against human prostate carcinoma PC-3 cells. KR28 induces apoptosis of PC-3 cells via ROS-mediated c-Abl upregulation, to activate p38 MAPK/ATF-2, which enhances RhoB expression.

Materials and Methods

Materials

All chemicals were dissolved in dimethyl sulfoxide (DMSO) as 10.0 mM stock solutions. Sulforhodamine B (SRB), N-acetylcysteine (NAC), SB253580 (p38 MAPK inhibitor), LY294002 (PI3 K inhibitor), and 2-,7-dichloro-fluorescein diacetate (DCF-DA) were purchased from Sigma-Aldrich (St. Louis, MO, USA). A protease inhibitor cocktail was obtained from Roche Applied Science (Indianapolis, IN, USA).

Cell culture

Cancer cell lines used are as follows: HeLa (cervical), HCT116 (colorectal), HCT15 (colorectal), MDA-MB-231 (breast), MDA-MB-435 (melanoma), A549 (non-small cell lung), NCI-H23 (non-small cell lung), LNCap (prostate), DU145 (prostate), PC-3 (prostate), ACHN (renal), and NUGC-3 (stomach). WI-38 cells (human fetal lung fibroblasts) were also used. Cells were maintained in RPMI 1640 containing 10 % [v/v] heat-inactivated fetal bovine serum, 100 units/ml penicillin, 100 µg/ml streptomycin, and 0.25 µg/ml amphotericin B at 37 °C in a humidified incubator with 5 % CO_2. Cell lines were procured from the Cancer Bank and Preclinical Research Program at the Korea Research Institute of Bioscience & Biotechnology (Daejeon, Korea).

Sulforhodamine B (SRB) Assay

The growth inhibition of cells in the presence of KR28 was measured by SRB assay as described [19]. SRB dye bound to cell matrix was quantified by spectrophotometry at 530 nm.

Flow cytometry analysis

Cells treated with KR28 and/or various inhibitors were harvested at specified time points, and sub-G1 cell populations were determined by flow cytometry after propidium iodide staining of cells [20]. A FACScan Flow Cytometer (Becton Dickinson, San Jose, CA, USA) was used, with Modifit software (Verity Software House, Inc., Topsham, ME, USA) analysis of histograms.

Knockdown of gene expression using siRNA

Knockdown of genes using siRNAs was carried out as previously described [17]. The sequences of siRNAs used are as follows: scrambled siRNA, 5′-CCUACGCCACCAAUUU CGUdTdT-3′ siRhoB1, 5′-CCGUCUUCGAGAACUAUGU dTdT-3′ sic-Abl, 5′-GAAACAAUGUUCCAGGAAdTdT-3′ sip38, 5′-CAAAUUCUCCGAGGUCUAAdTdT-3′ siATF2, 5′-GAUCAUUUGGCUGUCCAUAdTdT-3′. For each of the above, a total of 20 nM of siRNA was transfected into PC-3 cells per manufacturer's protocol. After a 36-h incubation period, the cells were treated with 5 µM KR28 and incubated for another 12–18 h. The knockdown of genes was analyzed by RT-PCR or Western blot analysis.

Western blot analysis

Cells were harvested in a RIPA buffer, lysed by sonication in ice, and used for Western blot analysis [17]. Mouse monoclonal antibodies (mAbs) to RhoB and rabbit polyclonal

antibodies to c-Abl, Bax, ATF-2, and p27 were purchased from Santa Cruz Biotechnology (Santa Cruz, CA, USA). Rabbit polyclonal antibodies to p38 MAPK, pRb, p-Thr-308-Akt, p-Ser-473-Akt, Akt, Bcl-2, PARP, caspase-3, GAPDH, and β-actin were supplied by Cell Signaling (Danvers, MA, USA). Rabbit polyclonal antibodies to ß-tubulin and Mouse mAb to p-Bad and goat polyclonal antibody to Bad were purchased from Abcam (Hanam-city, Korea) and Upstate Biotechnology, Inc. (San Diego, CA, USA), respectively.

Reactive oxygen species (ROS) assay

Intracellular production of ROS was detected by oxidation of 2-7-dichlorofluorescein diacetate (DCF-DA; Sigma-Aldrich) to fluorescent DCF by H_2O_2. Cells were grown to 80 % confluence and incubated with KR28 for 1–3 h in the presence or absence of NAC, a ROS scavenger. After incubation, cells were treated with DCF-DA (10 µM) for 30 min. Relative fluorescence was measured using a fluorescence plate reader Victor3 (Perkin Elmer Life Science, Waltham, MA) at excitation and emission wavelengths of 485 and 528 nm, respectively.

Nuclear and cytoplasmic fractionation

Nuclear and cytosolic fractionation was performed as described by Dignam et al. [21]. The cells were washed, suspended in ice-cold harvest buffer (10 mM HEPES pH 7.9, 50 mM NaCl, 0.5 M sucrose, 0.1 mM EDTA, 0.5 % Triton X-100 containing protease inhibitors), and incubated for 5 min on ice. The nuclei were separated by centrifugation, and the supernatant (cytosolic fraction) was transferred to a new tube. The nuclear pellet was washed, resuspended, and centrifuged, and the supernatant (nuclear fraction) was harvested.

Expression of GFP-RhoB

Wild-type RhoB gene was fused to green fluorescent protein (GFP) as pcDNA-DEST53E-RhoB. PC-3 cells were transfected with the pcDNA-DEST53E-RhoB vector using PolyFect (Qiagen Inc. Valencia, CA, USA.), and GFP-RhoB was assessed by fluorescence microscopy (Olympus, IX71 inverted microscope) as previously described [17, 22].

Luciferase assay

A cell-based RhoB-luciferase assay was performed in the cells transfected with pGL-RhoB-luciferase as described using a dual luciferase reporter system (Promega, Madison, WI, USA) [17]. Luciferase activity was integrated over a 10-second period and measured by luminometer (Victor X Light; Perkin Elmer, Waltham, MA, USA). Results were normalized to Renilla luciferase activity.

Human prostate cancer xenografts in athymic mice

The animal experiment was approved by the Institutional Animal Care and Use Committee, Korea Research Institute of Bioscience and Biotechnology (Daejeon, Korea). The pathogen-free BALB/CAnCrj-nu/nu female athymic nude mice aged 6–8 weeks (Charles River, Japan) were adapted to the sterile basic supplementary diet and acclimated to laboratory conditions for 1 week. For xenograft assay, PC-3 cells (3×10^7/mouse) were injected into the right flank subcutis of six nude mice. When approximate, mean tumor size of 100 mm³ was reached, and intraperitoneal KR28 (10 and 30 mg/kg/day, QD) and doxorubicin (2 mg/kg/day, Q2D) were administered for 14 days. On the final day, tumors were excised and analyzed to calculate the total tumor growth inhibition (TGI). Tumor volume (V) was computed as the following: V = (L × W2) × 0.5, where L and W represent maximum and minimum tumor dimensions, respectively. TGI outcomes were also subjected to ANOVA, followed by Dunnett's pairwise t test [23]. A p value of <0.05 marked statistical significance. All data are expressed as mean ± SD.
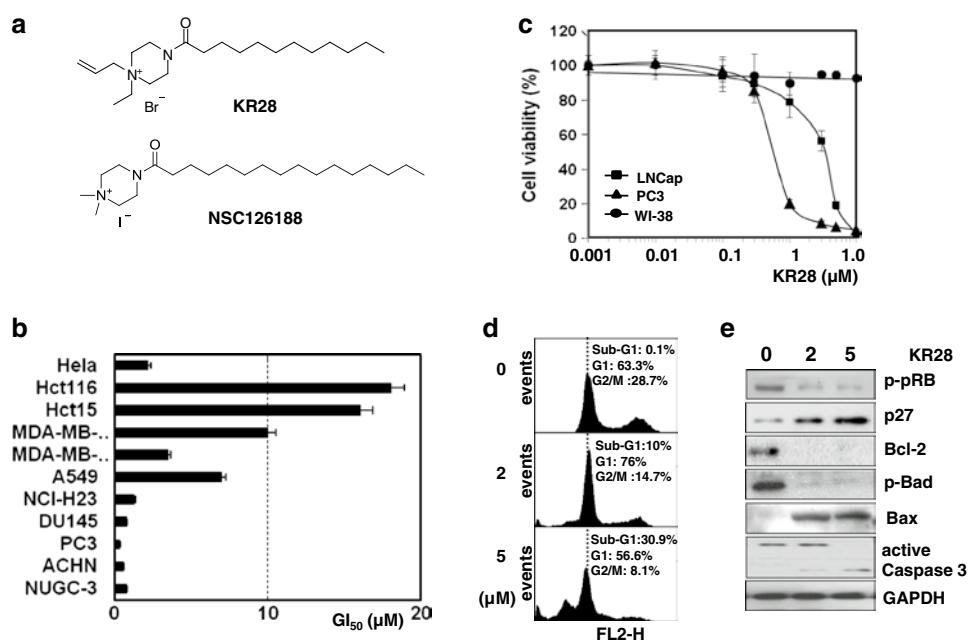
Statistical analysis

All data were obtained from three independent experiments. Statistical analysis was performed by Student's t test, and ANOVA, and followed by Dunnett's pairwise t-test. Values are presented as means and standard deviation (SD). Bars indicate SD. *$p < 0.01$, **$p < 0.05$, and ***$p < 0.005$.

Results

KR28, a novel compound, causes growth inhibition of PC-3 cells

A novel anticancer agent, KR28, a NSC126188 derivative (Fig. 1a), was synthesized in a two-step process: (1) condensation reaction of dodecanoic acid and N-ethylpiperazine and (2) N-allylation of the intermediate with allyl bromide. NSC126188 caused growth inhibition of most cancer cell lines tested, with a GI50 range of 0.5–3.0 µM [18]. However, KR28 showed differential sensitivity to cancer cell lines: PC-3 ($GI_{50} = 0.5$ µM), DU145 ($GI_{50} = 0.96$ µM), and NUGC-3 cells ($GI_{50} = 1.1$ µM) were more sensitive to KR28 than HCT116 ($GI_{50} = 18$ µM) and MDA-MB-231

cells (GI$_{50}$ = 10 µM) (Fig. 1b). Likewise, androgen-independent PC-3 cells (GI$_{50}$ = 0.5 µM) displayed more sensitivity to KR28 than androgen-dependent prostate cancer LNCap cells (GI$_{50}$ = 3.5 µM) (Fig. 1b, c). On the other hand, KR28 had a negligible effect on the growth of WI-38 (human fetal lung fibroblast) cells, implying selectivity of KR28 for malignant cells (Fig. 1c). Therefore, PC-3 cells were used to study mode of action of KR28. DNA fingerprinting of PC-3 cells was tested using AmplFLSTR profiler PCR amplification kit by the Korean Cell Line Bank.

KR28 induces apoptosis of PC-3 cells via G1 arrest

Flow cytometry was used to measure the apoptotic effect of KR28 on PC-3 cells (Fig. 1d). Eighteen hours after treatment with 2 µM of KR28, cells at G1 phase increased from 63.3 to 76 %, while the population of sub-G1 cells rose from 0.2 to 10 %. At 5 µM of KR28, sub-G1 cells climbed to 30.9 %, indicating increase in apoptosis. Western blots of proteins involved in cell cycle arrest and apoptosis were investigated (Fig. 1e). We found an increase in p27 expression and reduced phosphorylation of pRb. A decrease in Bcl-2 expression also occurred, indicating a suppression of survival signal transduction. Furthermore, Bax expression increased and dephosphorylation of Bad occurred, triggering binding of Bad to Bax [24]. These findings support that KR28 causes apoptosis of PC-3 cells via transient G1 arrest as shown in Fig. 1d.

KR28 induces ROS-mediated apoptosis of PC-3 cells

To elaborate upon KR28-induced apoptosis, we tested various inhibitors for potential inhibition of KR28-mediated apoptosis of PC-3 cells (Fig. 2a, b). When cell growth was measured in the presence of inhibitors, we found that N-acetylcysteine (NAC) and SB253580 rescued apoptotic cells by 84 and 62 %, respectively, compared with KR28 treatment only (Fig. 2a). By flow cytometry, sub-G1 cells were at 31.45 % in the presence of KR28, indicating decisive apoptosis. However, NAC, ROS scavenger, reduced sub-G1 apoptotic cells to 6.37 % (Fig. 2b), underscoring that apoptosis with KR28 was ROS-mediated. SB253580, a p38 MAPK inhibitor, also suppressed apoptosis by KR28 to 19.72 %, while LY294002, a PI3 K inhibitor, did not. It is expected that NAC works at upstream compared with SB203580 because NAC inhibited ROS and SB203580 inhibited p38 pathway, one of the downstream targets of ROS. Thus, ROS signaling to induce apoptosis of PC-3 cells likely proceeded in part through p38 MAPK.

To confirm the role of ROS in apoptosis, we measured intracellular production of ROS following KR28 treatment by the oxidation of DCF-DA to fluorescent DCF. DCF fluorescence increased 1 and 3 h after the treatment of PC-3 cells with KR28 (Fig. 2c). In addition, the elevated DCF fluorescence by KR28 dramatically decreased when PC-3 cells were treated with NAC, indicating ROS production in response to KR28 (Fig. 2d). We next investigated the relevance of growth inhibition and ROS production (Fig. 2e). The KR28-sensitive cells, PC-3, DU145, and NUGC-3, demonstrated a dramatic increase in DCF fluorescence following KR28 exposure compared with HCT116 and WI-38 cells, which were less responsive to KR28. Accordingly, ROS induction appears critical in KR28-mediated apoptosis of PC-3 cells.
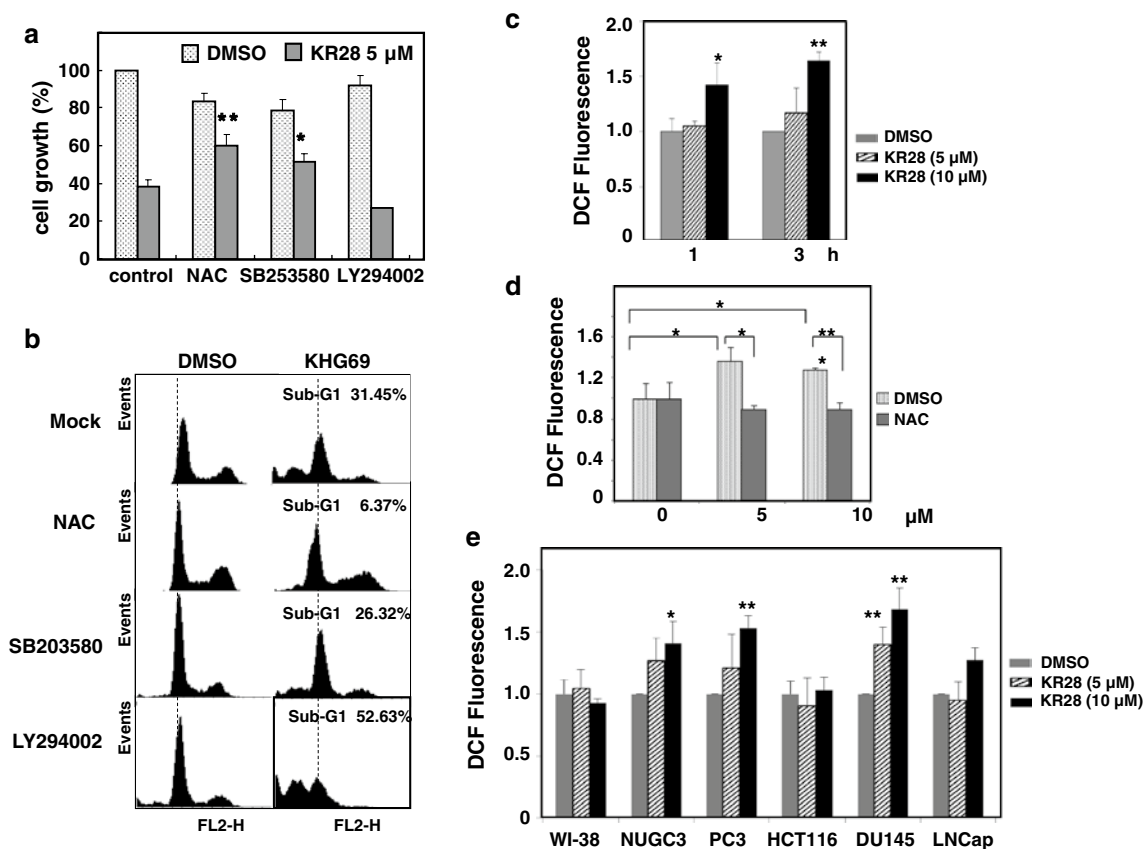
Fig. 2 Effect of inhibitors on KR28-induced apoptosis and induction of reactive oxygen species. Cells were treated with KR28 (5 μM) and inhibitors for 18 h. NAC (10 μM), SB253580 (10 μM), SP600125 (10 μM), and LY294002 (10 μM) were used. **a** Relative growth inhibition of cells. *p* values were determined by Student's *t* test. *Bars* indicate SD. *$p < 0.05$, **$p < 0.01$. **b** Flow cytometry analysis. PC-3 cells were fixed and stained with propidium iodide solution for FACS analysis. **c** Measurement of ROS in cells with KR28 (0, 5, 10 μM) for 1 and 3 h. The amount of fluorescent DCF produced in the control was set as 1. *p* values were determined by Student's *t* test. *Bars* indicate SD. *$p < 0.05$, **$p < 0.01$, ***$p < 0.005$. NT stands for "no treatment." **d** Inhibition of ROS production by NAC (10 μM) in the presence of KR28 (0, 5, 10 μM) for 3 h. **e** Production of ROS in various cancer cell lines treated with KR28 (0, 5, 10 μM) for 3 h

KR28 induces RhoB-mediated apoptosis via the c-Abl/p38 MAPK pathway

As further investigation into ROS-mediated apoptosis of KR28, we found that c-Abl expression markedly increased in a dose-dependent manner (Fig. 3a). Cell fractionation showed that nuclear c-Abl increased, supporting the role of nuclear c-Abl in the induction of apoptosis (Fig. 3b). Activation of c-Abl/p38 MAPK signaling induces expression of RhoB, a tumor suppressor rendering apoptosis of cancer cells. As such, mRNA and protein levels of RhoB increased in KR28-treated cells. Conversely, expression of both c-Abl and RhoB was reduced with NAC during KR28 exposure, suggesting that ROS induced by KR28 increases RhoB expression through c-Abl/p38 MAPK signaling (Fig. 3c).

RhoB expression was examined by siRNA knockdown of c-Abl, p38 MAPK, and ATF2. c-Abl knockdown reduced phosphorylation of p38 MAPK and RhoB expression (Fig. 3d). Knockdown of p38 MAPK or ATF2 decreased RhoB expression in the presence of KR28 (Fig. 3e, f). We similarly addressed whether knockdown of RhoB, c-Abl, or p38 MAPK could suppress apoptosis of PC-3 cells in the presence of KR28 (Fig. 3g). In fact, about 40–55 % of cells were rescued from apoptosis, indicating that c-Abl/p38/ATF2 signaling does regulate KR28-mediated apoptosis.

Next, we confirmed the effects of a transient RhoB expression on apoptosis of PC-3 cells. In the flow cytometry analysis, 38.72 % sub-G1 portion was detected in GFP-RhoB-expressed cells, while 5.12 % sub-G1 in control cells expressing GFP only (Fig. 4a). As expected, growth of cells expressing wild-type GFP-RhoB was greatly inhibited (Fig. 4b). This result clearly demonstrates that upregulation of RhoB results in apoptosis of PC-3 cells.

Finally, we assessed whether KR28 induced growth inhibition through increasing RhoB expression (Fig. 4c). Even with different basal expression levels of RhoB in cells, RhoB expression increased by KR28 more than twofold in
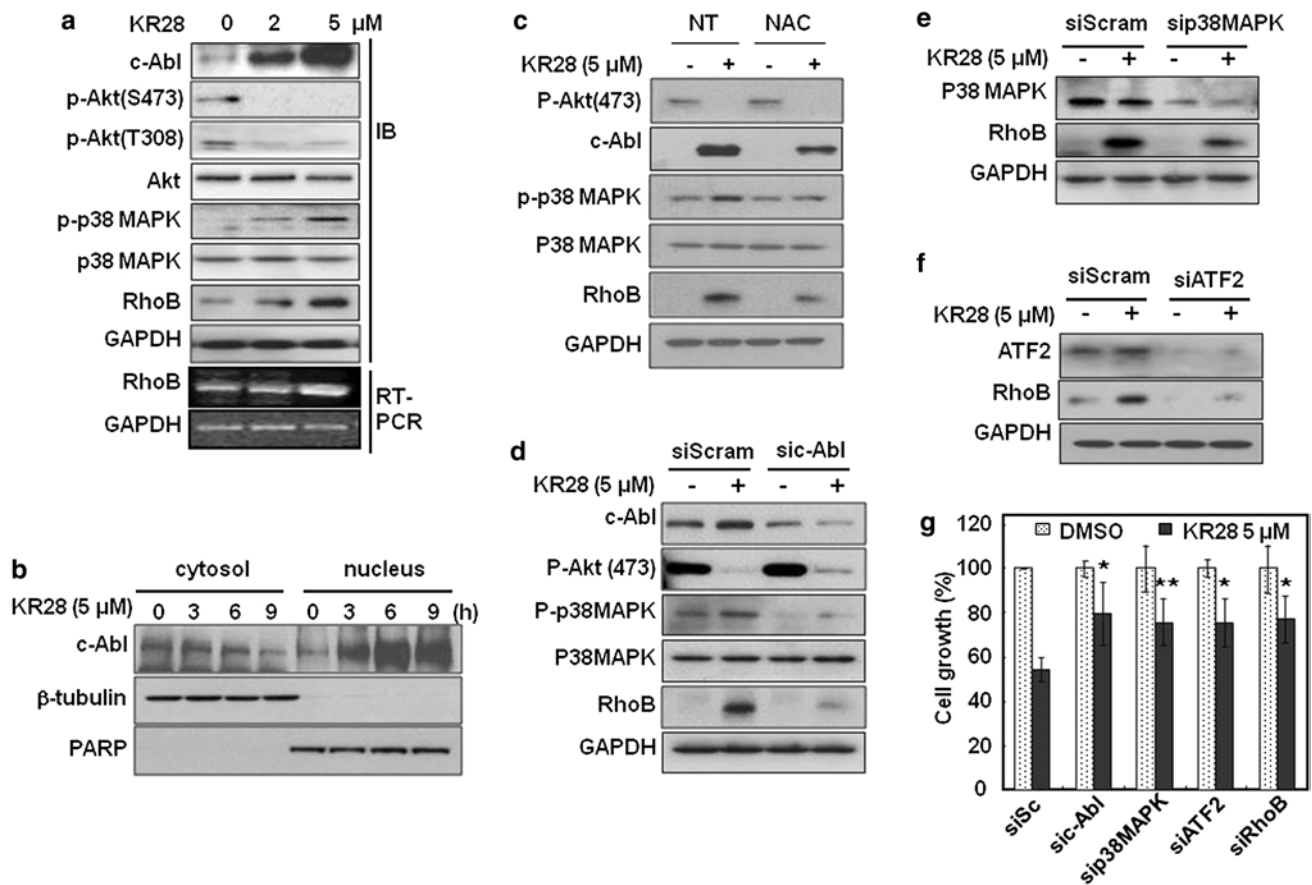
Fig. 3 Expression of RhoB via c-Abl/p38 MAPK signaling in KR28-induced apoptosis. **a** Western blot analysis of cells treated with KR28 (0, 2, 5 µM) for 12 h. **b** Localization of c-Abl. **c** Effect of NAC (10 µM) on the cells treated with KR28 (5 µM) for 12 h. **d–g** The effect of knockdown of c-Abl/p38 MAPK genes during KR28 treatment. The cells transfected with siRNA (20 nM each) for 36 h and treated with KR28 (5 µM) for another 12 h were compared by Western blot analysis (**d–f**) and SRB assay (**g**). The siRNAs used were siScram (control), sic-Abl (c-Abl siRNA), sip38(p38 siRNA), and siATF2 (ATF2 siRNA). Growth inhibition was determined by SRB assay and repeated three times. *p* values were determined by Student's *t* test. *Bars* indicate SD. *$p < 0.05$, **$p < 0.01$

PC-3, NUGC-3, and DU145 cells, which were sensitive to KR28 (Fig. 1b). In comparison, RhoB expression hardly increased in WI-38, A549, HCT116, and LNCap cells, which were less responsive to KR28. Therefore, RhoB expression may be correlated with ROS production because KR28-sensitive cells increase ROS following KR28 exposure (Fig. 2e). This result implicates that dramatic increase in ROS production is associated with RhoB expression and growth inhibition of cancer cells in the presence of KR28.

KR28 activates transcription RhoB via ROS signaling

To investigate the precise mechanism of RhoB expression by ROS in PC-3 cells, we performed reporter assays using various RhoB promoter constructs (Fig. 5a). When the −185 construct, containing the p300 binding site and two CCAAT boxes, was assayed in cells treated with KR28, RhoB promoter activity increased 15- to 20-fold (Fig. 5). However, construct −90 significantly reduced

RhoB promoter activity, dignifying that the p300 binding site is critical in regulating RhoB expression by KR28. The importance of the CCAAT and iCCAAT sequences was demonstrated by completely diminished RhoB promoter activity in the −21 construct. Reduced rates of RhoB-luciferase activity in −90 and −21 constructs, as opposed to the −185 construct, were 41.2 and 51.2 %, respectively. Evidently, both sites are equally important in activating RhoB transcription.

The inhibitory effects of NAC, SB253580, and ATF2 knockdown on −185 and −90 constructs were compared to analyze the regulation sites for RhoB expression. In the presence of NAC, luciferase activity in the −185 construct was inhibited by 70.4 % (Fig. 5b, e). Luciferase activity in the −90 construct, containing deletion of p300 binding site, was likewise reduced by 36.0 % with NAC. Apparently, the ROS generated by KR28 increased RhoB expression through both p300 binding site and CCAAT boxes. When the RhoB-luciferase assay was carried out using a p38
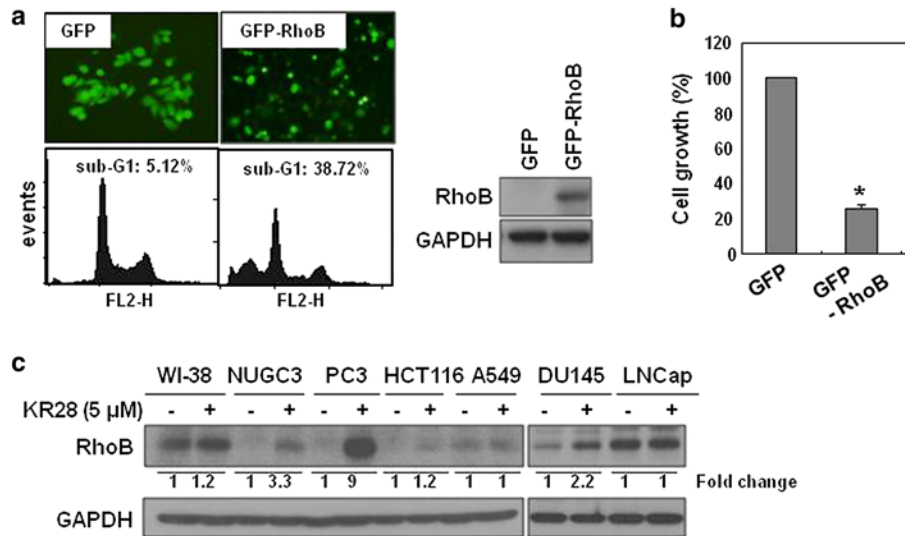
Fig. 4 Effect of RhoB expression on cell growth. **a** Effect of transient expression of GFP-RhoB on cell growth. The cells transfected with GFP-RhoB and incubated for 48 h were compared with control (GFP) by microscopy (**a**) and flow cytometry (**a**). **b** Growth inhibition of cells overexpressing GFP-RhoB was determined by SRB assay three times. *p* values were determined by Student's *t* test. *Bars* indicate SD. *$p < 0.05$. **c** Upregulation of RhoB by KR28 in various cancer cells. The changes in RhoB expression treated with 5 µM KR28 for 18 h were examined by Western blot analysis. Fold changes were indicated

Fig. 5 Cell-based RhoB-luciferase reporter assay. The transfected cells were preincubated with inhibitor for 2 h and treatment with 5 µM KR28 for 12 h. **a** Diagram of RhoB-luciferase reporter system. **b** Effect of NAC (10 µM) on RhoB promoter activity. **c** Effect of SB253580 (10 µM) on RhoB expression. **d** Effect of ATF2 knockdown on RhoB expression. **e** Relative RhoB-luciferase activity in −185 and −90 constructs. The effect of inhibitors, NAC, SB253580, and siATF-2 on RhoB expression was compared. *p* values were determined by Student's *t* test. *Bars* indicate SD. *$p < 0.05$, **$p < 0.01$
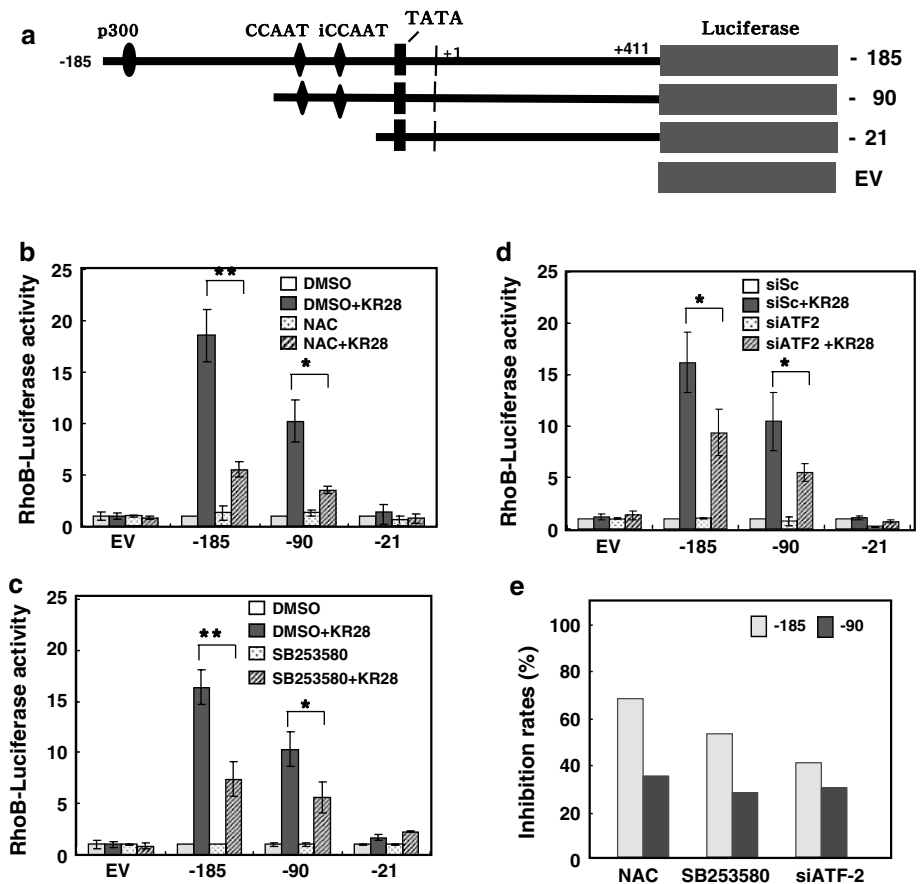
MAPK inhibitor, a similar result was obtained. The inhibition rates of luciferase activity by SB253580 were 54.9 and 28.7 % in the −185 and −90 constructs, respectively (Fig. 5c, e). It is clear that transcriptional inhibition by a p38 MAPK inhibitor was consequently mediated via the p300 binding site and CCAAT boxes. However, knockdown of ATF-2 reduced RhoB-luciferase activity by 42.0 and 30.9 % in the −185 and −90 constructs, respectively (Fig. 5d, e), with much less effect on −185 construct than NAC or p38 MAPK inhibitor exposure. It seems that ATF2 binds mostly to the CCAAT site to increase RhoB gene expression, whereas both NAC and the p38 MAPK inhibitor involve p300-binding-site- and CCAAT-mediated regulation. Taken together, both the p300 binding site and CCAAT boxes are major regulation sites of RhoB expression by ROS activation through c-Abl/p38 MAPK/ATF2 in PC-3 cells.

KR28 demonstrates in vivo antitumor efficacy in human cancer xenografts

The in vivo efficacy of KR28 was evaluated by tumor xenograft assay using Balb/c nude mice injected with PC-3 cells (Fig. 6). When mice with tumors approximating 100 mm^3 were given intraperitoneal KR28, solid tumor growth was inhibited in a dose-dependent manner without significant reduction in body weight (Fig. 6a). KR28 at doses of 10 and 30 mg/kg/day reduced PC-3 tumors by 32.3 and 74.7 %, respectively, compared with vehicle-treated controls, without apparent adverse effects (Fig. 6b–d). Doxorubicin, an anticancer drug used in the clinic, reduced a tumor size by 55.0 % at 2 mg/kg.

Discussion

Herein we have described KR28, a novel alkylpiperazine derivative, as an antitumor lead compound. Based on the structure of NSC126188, KR28 was designed and synthesized with two major modification points: shorter chain length of aliphatic carbon and introduction of larger size of substituent on piperidine group of NSC126188. For the effects of chain length, the analogues with 12–16 carbon chain length exhibited generally potent growth inhibitory profiles compared to NSC126188 in PC-3 and NUGC-3 cell lines. Replacements of methyl substituent on piperidine ring for allyl induced remarkably potent growth inhibitory activity in most of the tested human cancer cell lines except HCT-15 cell lines. It seemed to prefer the bulkier substituents for better antiproliferative activities due to higher lipophilicity and cell membrane permeability [25].

KR28 induces apoptosis, inhibiting the growth of PC-3 human prostate cancer cells. Its strong in vivo antitumor activity attenuated total tumor growth by up to 74.7 % in a mouse xenograft assay, without severe side effects.

We have determined that KR28 generated ROS, which increased nuclear c-Abl expression. Knockdown of c-Abl reduced p38 MAPK activation, as does SB253580, suppressing KR28-mediated apoptosis. In the presence of KR28, p38 MAPK activation induced p53-independent

Fig. 6 The in vivo antitumor efficacy of KR28 in xenograft assay. Drug treatment was initiated on the day when mean tumor size reached approximately 100 mm^3. KR28 (10, 30 mg/kg/day, QD) and doxorubicin (Doxo; 2 kg/day, Q2D) were administered intraperitoneally. **a** Body weight changes in the mice. **b** Tumor growth inhibition by KR28. Student's *t* test: *$p < 0.05$, **$p < 0.01$, ***$p < 0.005$. V.C.: Vehicle control. a$\Delta t = Vt - Vo$, Vt (measurement of the tumor volume), Vo (initial tumor volume). bIR: inhibition rate. **c** Comparison of tumor weights. **d** Picture of tumor tissues
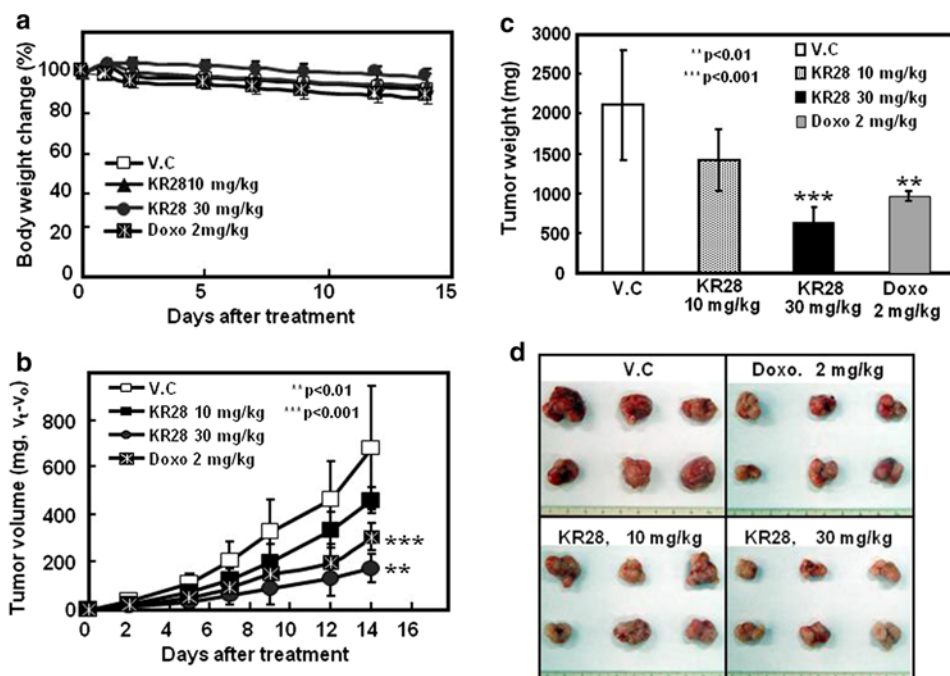
apoptosis of PC-3 cells. Phosphorylated p38 MAPK activates ATF2 to transactivate RhoB, which is crucial for apoptosis of PC-3 cells (SFig. 1). Interestingly, JNK signaling apparently is not required for KR28-mediated RhoB expression in PC-3 cells, because a JNK inhibitor could not rescue cells from apoptosis.

RhoB is regulated at the level of transcription. The p300 binding site and two CCAAT boxes in the RhoB promoter are important in this regard. Inverted CCAAT (i.e., ATTGG), which is located close to the functional TATA box, is essential for the induction of RhoB by UV light and MMS. Our study suggests that ROS produced by KR28 increases RhoB expression via the p300 binding site and CCAAT boxes. Treatment with an ROS scavenger and a p38 MAPK inhibitor decreased activation of RhoB through p300 binding site and CCAAT boxes, at the level of the transcription complex. It seems that ATF2 activity at the CCAAT site is largely responsible for the increase in RhoB expression. So far, no clear evidence has demonstrated how p300 binding site is involved in the transcription of RhoB even though there are several reports of CCAAT boxes for its role in transcriptional regulation of RhoB. We are studying recruitment of p300 and its partners to the p300 binding site to transcribe RhoB in cancer cells. Therefore, other signals activating p300 and its partners may affect transcription of RhoB in addition to c-Abl/p38 MAPK. A detailed investigation into KR28 induction of RhoB expression is currently underway.

It is not clear how RhoB induces apoptosis in cancer cells. The RhoB-mDia pathway may play a critical role in the cell death mechanism engaged by farnesyltransferase inhibitors [26]. Previously, we demonstrated that RhoB interacts with TNFAIP1, a TNFα-induced protein containing the BTB/POZ domain, which causes apoptosis of HeLa cells [22]. Furthermore, SAPK/JNK signaling may be involved in the apoptotic response induced by RhoB-TNFAIP1 interactions.

KR28 showed higher cytotoxicity to androgen-independent PC-3 and DU145 cells, which generated ROS, than to androgen-sensitive LNCap cells. The activated p38 MAPK clearly enhanced RhoB expression in PC-3 and DU145 cells (SFig. 2). However, neither activation of p38 MAPK nor increase in RhoB expression occurred in LNCap cells, in which Akt was highly phosphorylated. Furthermore, we found that KR28 showed higher cytotoxicity to PC-3 and NUGC-3 cells than to HCT116 cells. PC-3 and NUGC-3 cells demonstrated increased ROS production and RhoB expression following KR28 exposure compared with HCT116. It is likely that the increase in ROS may provide clues to the induction of apoptosis by KR28 with respect to RhoB expression. Therefore, RhoB expression as a function of KR28 treatment may well form the basis for defining the impact of ROS and provide clues to cell line specificity of KR28 anticancer therapy.

In summary, we maintain that KR28, a novel piperazine alkyl derivative, induces apoptosis of PC-3 prostate cancer cells via ROS-mediated RhoB expression through activation of the c-Abl/p38 MAPK pathway. KR28 has demonstrated strong in vivo antitumor activity in a mouse xenograft model, suggesting as a potential lead compound in cancer therapeutics. This finding is important developing strategy of ROS-induced RhoB expression to cause growth inhibition of cancer cells in anticancer therapy.

Conflict of interest None.

References

1. Wu WS (2006) The signaling mechanism of ROS in tumor progression. Cancer Metastasis Rev 25:695–705
2. Pelicano H, Carney D, Huang P (2004) ROS stress in cancer cells and therapeutic implications. Drug Resist Updat 7:97–110
3. Brandon M, Baldi P, Wallace DC (2006) Mitochondrial mutations in cancer. Oncogene 25:4647–4662
4. Pan J, She M, Xu ZX, Sun L, Yeung SC (2005) Farnesyltransferase inhibitors induce DNA damage via reactive oxygen species in human cancer cells. Drug Resist Updat 65:3671–3681
5. Kharbanda S, Ren R, Pandey P, Shafman TD, Feller SM, Weichselbaum RR, Kufe DW (1995) Activation of the c-Abl tyrosine kinase in the stress response to DNA-damaging agents. Nature 376:785–788
6. Yuan ZM, Huang Y, Whang Y, Sawyers C, Weichselbaum R, Kharbanda S, Kufe D (1996) Role for c-Abl tyrosine kinase in growth arrest response to DNA damage. Nature 382:272–274
7. Kharbanda S, Yuan ZM, Weichselbaum R, Kufe D (1998) Determination of cell fate by c-Abl activation in the response to DNA damage. Oncogene 17:3309–3318
8. Kralova J, Dvorak M, Koc M, Kral V (2008) p38 MAPK plays an essential role in apoptosis induced by photoactivation of a novel ethylene glycol porphyrin derivative. Oncogene 27:3010–3020
9. Scheijen B, Griffin JD (2002) Tyrosine kinase oncogenes in normal hematopoiesis and hematological disease. Oncogene 21:3314–3333
10. Mazieres J, Antonia T, Daste G, Muro-Cacho C, Berchery D, Tillement V, Pradines A, Sebti S, Favre G (2004) Loss of RhoB expression in human lung cancer progression. Clin Cancer Res 10:2742–2750
11. Adini I, Rabinovitz I, Sun JF, Prendergast GC, Benjamin LE (2003) RhoB controls Akt trafficking and stage-specific survival of endothelial cells during vascular development. Genes Dev 17:2721–2732
12. Prendergast GC (2001) Actin' up: RhoB in cancer and apoptosis. Nat Rev Cancer 1:162–168
13. Huang M, Prendergast GC (2006) RhoB in cancer suppression. Histol Histopathol 21:213–218
14. Kim CH, Won M, Choi CH, Ahn J, Kim BK, Song KB, Kang CM, Chung KS (2010) Increase of RhoB in gamma-radiation-induced

apoptosis is regulated by c-Jun N-terminal kinase in Jurkat T cells. Biochem Biophys Res Commun 391:1182–1186

15. Delarue FL, Adnane J, Joshi B, Blaskovich MA, Wang DA, Hawker J, Bizouarn F, Ohkanda J, Zhu K, Hamilton AD et al (2007) Farnesyltransferase and geranylgeranyltransferase I inhibitors upregulate RhoB expression by HDAC1 dissociation, HAT association and histone acetylation of the RhoB promoter. Oncogene 26:633–640

16. Fritz G, Kaina B (2001) Transcriptional activation of the small GTPase gene rhoB by genotoxic stress is regulated via a CCAAT element. Nucleic Acids Res 29:792–798

17. Kim BK, Kim HM, Chung KS, Kim DM, Park SK, Song A, Won KJ, Lee K, Oh YK, Lee K et al (2011) Upregulation of RhoB via c-Jun N-terminal kinase signaling induces apoptosis of the human gastric carcinoma NUGC-3 cells treated with NSC12618. Carcinogenesis 32:254–261

18. Kim BK, Kim DM, Chung KS, Park SK, Choi SJ, Song A, Lee K, Lee CW, Song KB, Han G et al (2011) NSC126188, a piperazine alkyl derivative, induces apoptosis via upregulation of RhoB in HeLa cells. Invest New Drugs 29:853–860

19. Kim DM, Koo SY, Jeon K, Kim MH, Lee J, Hong CY, Jeong S (2003) Rapid induction of apoptosis by combination of flavopiridol and tumor necrosis factor (TNF)-alpha or TNF-related apoptosis-inducing ligand in human cancer cell lines. Cancer Res 63:621–626

20. Chung KS, Yim NH, Lee SH, Choi SJ, Hur KS, Hoe KL, Kim DU, Goehle S, Kim HB, Song KB et al (2008) Identification of small molecules inducing apoptosis by cell-based assay using fission yeast deletion mutants. Invest New Drugs 26:299–307

21. Dignam JD, Lebovitz RM, Roeder RG (1983) Accurate transcription initiation by RNA polymerase II in a soluble extract from isolated mammalian nuclei. Nucleic Acids Res 11:1475–1489

22. Kim DM, Chung KS, Choi SJ, Jung YJ, Park SK, Han GH, Ha JS, Song KB, Choi NS, Kim HM et al (2009) RhoB induces apoptosis via direct interaction with TNFAIP1 in HeLa cells. Int J Cancer 125:2520–2527

23. Lee CW, Hong DH, Han SB, Jung SH, Kim HC, Fine RL, Lee SH, Kim HM (2002) A novel stereo-selective sulfonylurea, 1-[1-(4-aminobenzoyl)-2,3-dihydro-1H-indol-6-sulfonyl]-4-phenyl-imidazolidin-2-one, has antitumor efficacy in in vitro and in vivo tumor models. Biochem Pharmacol 64:473–480

24. Chen LH, Hsu CY, Weng CF (2006) Involvement of P53 and Bax/Bad triggering apoptosis in thioacetamide-induced hepatic epithelial cells. World J Gastroenterol 12:5175–5181

25. Yang JS, Song D, Lee B, Ko WJ, Park SK, Won M, Lee K, Kim HM, Han G (2011) Synthesis and biological evaluation of novel aliphatic amido-quaternary ammonium salts for anticancer chemotherapy: part I. Euro J Med Chem 46:2861–2866

26. Kamasani U, Duhadaway JB, Alberts AS, Prendergast GC (2007) mDia function is critical for the cell suicide program triggered by farnesyl transferase inhibition. Cancer Biol Thera 6:1422–1427